Journal of Experimental Botany, Vol. 55, No. 399, pp. 1061–1069, May 2004
DOI: 10.1093/jxb/erh118 Advance Access publication March 26, 2004

Journal of Experimental Botany

RESEARCH PAPER

Air volume measurement of 'Braeburn' apple fruit

Lazar Dražeta[1,2], Alexander Lang[1], Alistair J. Hall[1], Richard K. Volz[3] and Paula E. Jameson[2,*]

[1] *HortResearch, Private Bag 11 030, Palmerston North, New Zealand*

[2] *Institute of Molecular BioSciences, Massey University, Private Bag 11 222, Palmerston North, New Zealand*

[3] *HortResearch, Private Bag 1401, Havelock North, New Zealand*

Received 12 December 2003; Accepted 23 January 2004

Abstract

The radial disposition of air in the flesh of fruit of *Malus domestica* Borkh., cv 'Braeburn' was investigated using a gravimetric technique based on Archimedes' principle. Intercellular air volume was measured by weighing a small tissue sample under water before and after vacuum infiltration to remove the air. In a separate procedure, the volume of the same sample was measured by recording the buoyant upthrust experienced by it when fully immersed in water. The method underestimates tissue air volume due to a slight invasion of the intercellular air spaces around the edges of the sample when it is immersed in water. To correct for this error, an adjustment factor was made based upon an analysis of a series of measurements of air volume in samples of different dimensions. In 'Braeburn' there is a gradient of declining air content from just beneath the skin to the centre of the fruit with a sharp discontinuity at the core line. Cell shape and cell packing were observed in the surface layers of freshly excised and stained flesh samples using a dissecting microscope coupled to a video camera and a PC running proprietary software. Tissue organization changed with distance below the skin. It is speculated that reduced internal gas movement, due to the tightly packed tissue of 'Braeburn' and to the potential diffusion barrier at the core line between the cortex and the pith, may increase susceptibility of the flesh to disorders associated with tissue browning and breakdown.

Key words: Apple, Archimedes' principle, 'Braeburn', cell configuration, intercellular space, internal injury.

Introduction

An apple fruit is mainly composed of the flesh made of parenchyma tissue permeated with vasculature and intercellular air spaces (Esau, 1977). The volume of air increases during fruit growth and occupies a considerable proportion of the fruit at harvest (Bain and Robertson, 1951; Skene, 1966; Westwood *et al*., 1967; Soudain and Phan Phuc, 1979; Harker and Ferguson, 1988; Yamaki and Ino, 1992; Ruess and Stösser, 1993). This increase in air space is accompanied by a proportional decline in fruit density while the density of the fruit cells themselves remains roughly constant (Bain and Robertson, 1951; Skene, 1966; Westwood *et al*., 1967). Furthermore, the volume of the intercellular air spaces continues to increase during storage (Soudain and Phan Phuc, 1979; Hatfield and Knee, 1988; Harker and Hallett, 1992; Ruess and Stösser, 1993; Tu *et al*., 1996; Harker *et al*., 1999).

The fraction of intercellular air differs between cultivars (Reeve, 1953; Baumann and Henze, 1983; Vincent, 1989; Ruess and Stösser, 1993), and larger fruit of the same cultivar have a higher proportion of air than smaller ones (Reeve, 1953; Ruess and Stösser, 1993; Volz *et al*., 2004). Intercellular air volume is also important in understanding post-harvest quality. Fruit with greater fractional air volumes have been shown to be softer (Hatfield and Knee, 1988; Yearsley *et al*., 1997*a*, *b*; Volz *et al*., 2004), or more mealy (Harker and Hallett, 1992; Tu *et al*., 1996) and to have greater internal gas diffusion rates (Rajapakse *et al*., 1990).

A range of techniques has been developed to measure intercellular air in apple fruit. One is based on weighing the volume of water that replaces an equal volume of air removed by a vacuum from a submerged sample. A number of studies have used this principle with a range of sampling methods, vacuum pressures, treatment durations,

* To whom correspondence should be addressed. Fax: +64 6 350 5688. E-mail: P.E.Jameson@massey.ac.nz

and infiltration media (Reeve, 1953; Harker and Ferguson, 1988; Vincent, 1989; Rajapakse *et al*., 1990; Yamaki and Ino, 1992; Yearsley *et al*., 1996). By contrast, Calbo and Sommer (1987) estimated intercellular air volume using a gasometric technique that measured the amount of air extracted from samples when subjected to vacuum. An alternative way to calculate air fraction has been to assess the weight and volume of a whole fruit when immersed in water (Bain and Robertson, 1951; Skene, 1966; Westwood *et al*., 1967; Baumann and Henze, 1983; Hatfield and Knee, 1988; Harker and Hallett, 1992; Tu *et al*., 1996; Harker *et al*., 1999). Other authors have taken a stereological approach to estimate air volume (Soudain and Phan Phuc, 1979; Ruess and Stösser, 1993; Goffinet *et al*., 1995). However, estimates of air volume in apples in the studies above ranged widely (*c*. 2.5–41%).

The intent of this study was to develop a method so that internal air along the radius of the fruit could be accurately measured and the flesh structure at the cellular level could be assessed. A gravimetric approach based on Archimedes' principle was chosen, as this avoids assumptions and errors implicit in other methods. Particular attention has been paid to equilibration times, and corrections for surface effects, as in previous gravimetric studies these aspects have been neglected. 'Braeburn' was used as it is known to have a relatively dense and firm flesh (Dadzie, 1992; Yearsley *et al*., 1997*a*, *b*), poor flesh gas-diffusivity (Rajapakse *et al*., 1990), and low skin gas-permeance (Rajapakse *et al*., 1990; Dadzie, 1992). All these features could be related to its known susceptibility to internal tissue browning and breakdown.

Materials and methods

Plant material

The study used mature trees of 'Braeburn' apples grown at the Massey University Fruit Crops Unit, Palmerston North, New Zealand. Trees were planted on MM 106 rootstock and managed according to standard commercial practice. Fruit without obvious blemishes were picked at late commercial harvest. To minimize variation, fruit of similar size were chosen (*c*. 200–250 g). They were stored in a cool-store (0.5 °C, *c*. 95% RH) for up to five months pending analysis. Day-to-day storage was in a cold room (2 °C, no humidity control).

Air volume measurement

The intercellular air volume of freshly excised blocks of apple flesh was measured using methods based upon Archimedes' principle. The technique used two experimental arrangements involving electronic balances with a 1 mg sensitivity.

The first arrangement measured the volume of the sample by recording the buoyant upthrust experienced by a sample fully immersed in water (Fig. 1A). To do this, a small block of flesh was impaled on the tip of a fine (0.24 mm diameter) steel entomological pin and this attached to a magnet mounted on a light stand that rested on the bench. The components were so positioned that when attached to the magnet, the sample was held just beneath the surface of water that was contained in a small (50 cm^3) plastic container that rested on the pan of a pre-tared electronic balance. The buoyant upthrust

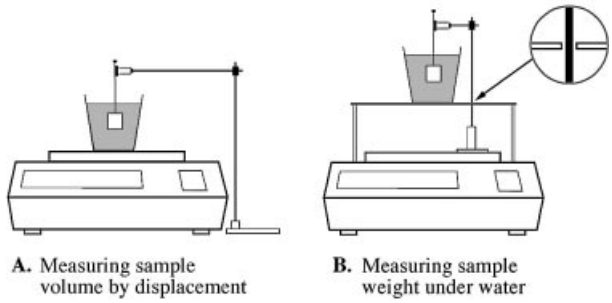

Fig. 1. Experimental arrangements for measuring fractional air volume. (A) Sample volume was first recorded by measuring the upthrust on the sample when fully immersed (equal to the weight of displaced water and expressed as an equal and opposite downthrust on the balance). (B) Sample air content was measured by weighing the same sample under water before and after vacuum air extraction.

experienced by the sample appears to the balance as an equal and opposite downthrust and is expressed as an apparent increase in the weight of the water in the container. Because the density of water at 20 °C is 0.99823 g cm^{-3}, the balance reading (g) can be directly interpreted as a sample volume (V) (cm^3). With a 1 mg sensitivity balance the procedure yields sample volume estimates to the nearest 1 µl. A wetting agent (0.1% Silwet L-77) was added to the water to help eliminate entrapment of air bubbles as the sample was immersed. The force of the meniscus acting upon the pin as it broke the surface (about 1 mg) was minimized both by the use of a fine pin and by the wetting agent.

A second balance arrangement was used to measure the air volume of the sample. This involved a subtle variation of the first (Fig. 1B). Here, the small container rested on a light 'bridge' mounted on the body of a similar pre-tared balance in such a way that the container was supported just *above* the pan. A similar magnet was mounted on a wire support and a light stand and this assembly rested on the balance pan. By attaching the pin holding the flesh sample to the magnet, the sample was again held just beneath the water. With this second arrangement, the balance recorded the weight of the sample while under water. By weighing the sample just before (W_1) and just after (W_2) the removal of tissue air under vacuum, it was possible to determine the volume of air extracted as an apparent increase in sample weight ($W_\Delta = W_2 – W_1$). Again, because the density of water is very close to unity, the difference in balance readings (g) can be interpreted directly as the volume of air removed by vacuum extraction (cm^3). A 1 mg sensitivity balance measures air volumes to the nearest 1 µl.

Air extraction (after the first weighing and before the second) was accomplished by transferring the sample, still with its pin, to a 50 cm^3 plastic vial of water containing 0.1% Silwet L-77. A small sinker weight made of a spiral of wire solder was threaded onto the pin to hold the sample beneath the water. While under water in this vial, the sample was exposed for 60 s to reduced atmospheric pressure of *c*. 2 kPa (vapour pressure of water at ≅20 °C). This caused the intercellular air, initially at atmospheric pressure (*c*. 100 kPa), to expand out through the cut tissue surfaces leaving only a small residue of air within the tissue (2 kPa/100 kPa or 2% of the initial amount). This small error is systematic and can either be ignored or allowed for in calculation if the temperature is known. Following release of the vacuum, the sample was held under the water for a further 60 s. This caused the residue of internal air to

contract and the internal spaces (previously air-filled) to became occupied with water (now at atmospheric pressure).

The fractional air content (A) of the sample (%) is, therefore, given as the difference between the two underwater weights expressed as a percentage of the sample volume

$$A = (W_\Delta/V)100 \quad (1)$$

Timings

A preliminary study showed that 60 s of air extraction (under vacuum) followed by 60 s of water replacement (at atmospheric pressure) was sufficient for most of the air in a 3×12×12 mm tissue block to be extracted and replaced by water. To determine *optimal* timings, equatorial discs (15–20 mm thick) were taken from several fruit. Disposable microtome blades (Leica Model 818) were used for excision of samples to minimize tissue damage close to the cut surfaces. The discs were cut so as to produce pairs of blocks 12×12×r mm with their r axes aligned with the fruit radius. One of each block pair was used as control (with fixed air-extraction and water-replacement timings) while the other was exposed to a range of timings. This plan allowed data to be normalized (i.e. to remove errors due to fruit:fruit and radial variability) by taking the ratio of air volume estimates for a pair of matched blocks (treatment/control).

To determine the optimum time for water replacement, the control blocks were exposed to 120 s of vacuum extraction and to 480 s of water replacement. Both these timings were judged to be longer than the times required for completion. To determine the optimal water-replacement timing, extraction times for the treatment blocks were fixed at 120 s (like the controls) while their changing weights (as they took up water) were recorded every 30 s until a steady-state was achieved (<480 s). Five replicate pairs of blocks of each of three sizes (r = 3, 6, and 12 mm) were used to assess the influence of sample size on water-replacement times.

Once the optimum water-replacement time had been determined (300 s for a 12×12×12 mm block), five replicate pairs of blocks were used to determine the optimal vacuum extraction time. Tested times were 5, 15, 30, 60, 120, 240, and 480 s. The control blocks were all extracted for 480 s.

Spatial distribution of intercellular spaces

Fruit were cut at the equator to excise transverse discs about 15–20 mm thick. Radial transects (12×12×r mm) were cut from these discs. Transects extended the full distance (*c.* 30 mm) from the skin to the fruit axis and included the primary (petal) bundle at the core line (Fig. 2A). To facilitate vacuum infiltration, the skin and the cartilaginous walls of the locules were shaved off very thinly. This radial transect was then sliced (blade aligned parallel to the skin) so as to create from it ten ≅3 mm thick blocks. Each series of 10 blocks provided the samples for measuring air volume change along a fruit radius.

To investigate the radial disposition of tissue air ten fruit were tested. One transect was taken from each fruit giving 100 blocks (ten replicates for each tissue depth). The volumes of intercellular air were combined across replicates for each tissue depth so as to yield a mean fractional air content (%) along the radii. Each transect contained eight rectangular 3×12×12 mm blocks (B_1 to B_8) plus two trapezoidal blocks close to the fruit axis (B_9 and B_{10}). These blocks were also 3 mm thick but their shape was dictated by the proximity of the locules (Fig. 2A). The significance of features of the radial pattern were tested using PROC GLM (SAS Institute Inc., 2000) with fruit included as a class variable.

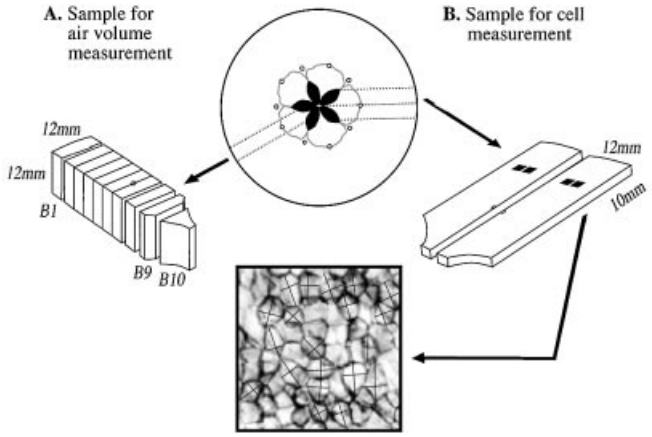

Fig. 2. Tissue sampling for air volume and cell measurements. A flesh disc about 15–20 mm thick was cut from the fruit equator. (A) Each transect (12×12×r mm) was subsequently cut into ten blocks for air volume measurement (note the trapezoidal shape of the two inner blocks, B_9 and B_{10}). (B) Five pairs of thin transects were also taken from one fruit and stained to reveal the walls of entire cells just beneath the surface. The two orthogonal diameters of 400 well-defined cells were randomly measured from two fields in the middle of the cortex for each transect.

Cell measurements

One fruit was cut transversely to form five pairs of flat equatorial transects (Fig. 2B) and these were rinsed briefly with water to remove cell-content residues from the cut surfaces. A ferric tannate staining (Goffinet *et al.*, 1995) was used to highlight cell walls exposed on the cut surfaces and stained cells were measured immediately to minimize possible dimensional change due to osmotic water uptake.

Cell dimensions were measured using a video-microscope system (a Wild M3Z dissecting microscope coupled to a JVC TK-1280E video camera and a PC running Video Master™ software). Transects were mounted under water to minimize light scattering from the irregular block surface. To stop transects from moving they were lightly impaled on a thin spike attached to the bottom of the dish. This arrangement presented a sharp image of whole cortical cells from just beneath the cut surface onto a 19" flat VDU screen at ×195 magnification. The software allowed measurement, using the mouse, of a live image and direct data acquisition to disc.

For each transect, cell dimensions (two orthogonal diameters) were obtained for 40 cells from two adjacent fields in the middle of the cortex, approximately 10 mm in from the skin (Fig. 2B). The first diameter measurement (d_1) was always made in line with the long axis of the cell and the second measurement (d_2) at right angles to this. For later calculations, the geometrical mean of these diameters (D) was calculated as

$$D = (d_1 d_2)^{0.5} \quad (2)$$

Adjustment for air loss

When a block of flesh is immersed in water there is a tendency for water to invade the air spaces near the cut surface. Air displaced in this manner at the initial weighing (W_1) is not recorded by this method, thus causing underestimation of air content. The magnitude of the error will depend on the surface area to volume ratio of the sample (and thus on its size and shape). This loss can be quantified, and corrected for, by considering it as equal to a loss of air in a superficial layer of thickness (T) all around the sample.

The value taken by T will likely be similar in the tangential directions (t) relating to the two transverse and two radial–longitudinal faces of a tissue block, but may be greater in the radial direction (t_x) relating to the two tangential block faces. This is because apple parenchyma is permeated with a network of air spaces radiating out from the centre of the fruit (Reeve, 1953; Vincent, 1989; Khan and Vincent, 1990).

It is unlikely that on sample immersion, water will invade an air space where the cut aperture to this space is smaller than its maximum diameter. For this to happen would require an increase in the area of the invading meniscus and thus the input of energy (e.g. from a vacuum pump). It is more likely that only those cut air spaces whose diameters *decrease* with depth will be invaded prior to evacuation. This insight leads to the hypothesis that in the two tangential directions, t will take a value equal to about one-quarter of the average cell diameter. Recall that, and with random sectioning, the air spaces between close-packed spheroidal cells will be so cut that either the aperture falls *before* the space's mid-point (in this case no air is lost), or it falls *after* the mid-point (in this case water enters freely and all air is displaced). Air spaces, having similar maximum dimensions to the spheroidal cells that form their boundaries, and these two scenarios occurring with the similar likelihood, it is likely that air loss will occur to a depth of a quarter-cell diameter. The conspicuous radial air channels of some cultivars may offer freer access to water invasion in the radial direction. In this case the effective thickness in this direction from which air is lost (t_x) may be greater.

To check these predictions, pairs of 12×12×12 mm blocks of cortical tissue (cut from 4–16 mm below the skin), were taken from a number of apples. The air volume of one block was measured intact while the air volume of the other was measured (by summing) after it had been cut up into a number of slices. Sixteen such pairs of blocks were measured. In six cases the sliced block was cut into two 6 mm slices, in four into three 4 mm slices, in three into four 3 mm slices, in two into six 2 mm slices, and in one into twelve 1 mm slices. For each pair, the sum of the air volumes in the slices (ΣV) was compared with the value for the paired intact block (V) where, because of the block 'edge' effect, $V > \Sigma V$. A model was then used to evaluate a correction factor (F) that takes as input the shape, size, and orientation of the block where

$$V_{\text{corrected}} = V_{\text{measured}} F \quad (3)$$

The error is expected to be inversely related to the size of the sample. The model was fitted by least squares using PROC NLIN (SAS Institute Inc., 2000).

Results

Timings

Plots of the relative air volume for blocks of different sizes and times are shown in Fig. 3. Data were normalized by dividing the air content value obtained for the matching block pair that had been exposed for times judged to be excessive (namely, 120 s for extraction and 480 s for water replacement). This creates the property that results in an asymptote to unity.

The largest blocks (12×12×12 mm) required 300 s for water replacement, 6×12×12 mm blocks required 120 s, and 3×12×12 mm blocks required just 30 s (Fig. 3A). Air extraction, however, even from the largest (12×12×12 mm) blocks was completed within about 60 s (Fig. 3B).

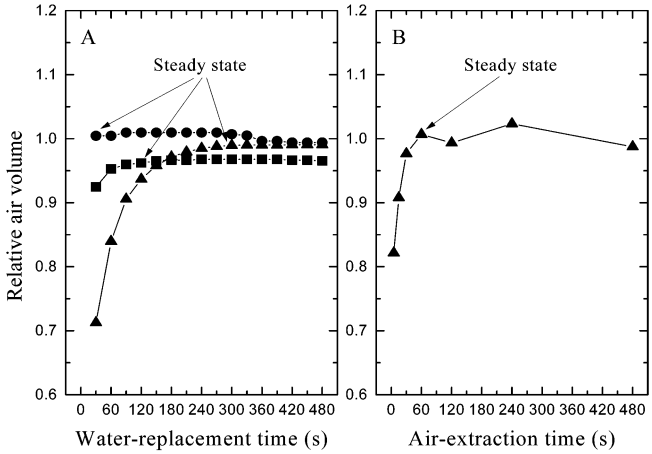

Fig. 3. Relative air volume during water replacement (A) and air extraction (B). The points are mean values (n=10) for block sizes 3×12×12 mm (circles), 6×12×12 mm (squares), and 12×12×12 mm (triangles).

Cell measurements

Notable differences existed between the two cell diameter measurements. For cells taken from the mid-cortex, the aspect ratio of the long to the short cell diameters averaged 1.44 (the mean cell length was 294 μm and the mean cell width was 205 μm). The geometrical mean diameter was thus calculated as 245±2 μm, which yields a mean cell volume of 0.0077 mm^3 (using $4/3\pi r^3$).

In 'Braeburn', the parenchyma cells of the cortex are large, thin-walled, irregular spheroids. They are usually slightly elongated along one axis and they have faceted surfaces. Also, at the tissue level, the alignment of their long axes appeared random (i.e. their alignment was *not* related to the major axes of the fruit). Intercellular air spaces were conspicuous and each cell could be seen to make contact with the walls of a number of adjacent cells. However, cell orientation and cell aspect ratio changed towards the centre of the fruit. Parenchyma cells of the pith were packed more closely, especially near to structures such as the locules and vascular bundles. Here, cells were grouped into compact radiating tiers and were elongated so as to be almost cylindrical in shape.

Adjustment for air loss

The prediction was that there would be a small loss of intercellular air from the edges of a flesh sample as it is immersed in water. This means that, when measuring the air content of a 12×12×x mm block, one is actually only measuring the air contained in a block that is 12–2t×12–2t×x–2t_x mm. Consider the ratio (y) of the air volume in a sliced 12×12×12 mm block with that in an intact block, which will be independent of t (the thickness from which air is lost from the transverse and longitudinal block faces). This ratio is given by

$$y = \frac{12}{12 - 2t_{12}} \frac{x - 2t_x}{x} \quad (4)$$

where t_x and t_{12} are the thicknesses from which air is lost from the tangential faces of blocks having radial dimensions of x mm and 12 mm, respectively.

First, consider the possibility that $t_x = t_{12}$. Here, the effective thickness from which air is lost from the tangential faces will be the same for all slice dimensions x. If all the data are grouped together and t_x is estimated using a least squares regression, the value $t_x = 0.154$ is obtained. This fixed T value does *not* fit the ratio data well (Fig. 4, dashed line). The idea of t_x being a constant is therefore untenable.

A more reasonable approach is to assume that t_x is relatively constant for large slice thicknesses, but as the slice dimension x, in the radial direction, reduces to zero, so does t_x. One way to describe such a relationship is by

$$t_x = t_{max}(1–\exp(–kx)) \quad (5)$$

where t_{max} and k are the parameters to be fitted. The ratio y is therefore given by

$$y = \frac{12}{12 - 2t_{max}\,(1 - \exp(-12k))} \frac{x - 2t_{max}\,(1 - \exp(-kx))}{x} \quad (6)$$

Fitting this equation to all 16 data points using a least squares regression gives $t_{max} = 0.292$ mm and $k = 0.544$ mm^{-1}. This fits the data reasonably well (Fig. 4, solid line). The calculated effective surface layer thickness ranges from 0.123 mm for a 1 mm slice to 0.281 mm for a 6 mm slice (Table 1), and the latter is close to the maximum value $t_{max} = 0.292$ mm. Hence, to allow for air loss from a sample surface on immersion in water, the air content measured in a rectangular $12 \times 12 \times x$ mm blocks (e.g. B_1 to B_8 in Fig. 2) should be corrected using F

$$F = \left[\frac{12}{12 - 2t} \frac{12}{12 - 2t} \frac{x}{x - 2t_x}\right] \quad (7)$$

where t is the effective thickness from which air is lost in the tangential direction (equivalent to about 0.25 of a cell diameter as predicted), and t_x can be calculated for any radial thickness from equation (5) and amounts to 0.235 mm for a 3 mm slice (equivalent to about one cell diameter).

The blocks bordering the locules (B_9 and B_{10}) are more difficult as they are 'trapezoidal' in shape. For simplicity, a similar approach can be applied, taking off a thickness t_x in the radial direction and t in the tangential direction (Fig. 5). Given the minimum (a) and maximum (b) widths of the trapezoid and the height (x), then assuming symmetry the correction factor becomes

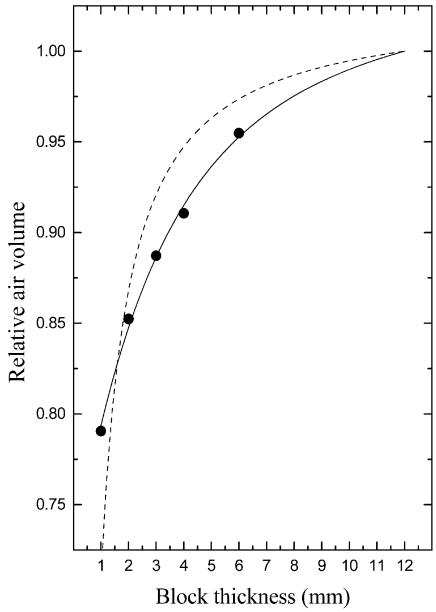

Fig. 4. Relative air volume in blocks of different radial dimensions. Each mean value (circles) represents normalized measurements for each block size. The lines were fitted using T value fixed (dashed line) and T value varying with block thickness (solid line).

Table 1. *Air loss in the radial direction* (t_x)*, (±SE) due to water invasion calculated using Equation 4*

The effective surface layer thickness from which air is lost due to water invasion was determined for blocks of different thickness (x).

Block thickness (x) (mm)	Effective surface layer thickness (t_x) (mm ±SE)
1	0.123±0.016
2	0.194±0.022
3	0.235±0.039
4	0.259±0.056
6	0.281±0.082

$$F_{trapezoid} = \left[\frac{0.5(a+b)}{\frac{1}{2}(a+b) - 2t[\sin(\theta)]^{-1}} \frac{12}{12 - 2t} \frac{x}{x - 2t_x}\right] \quad (8)$$

where

$$\tan(\theta) = \frac{2x}{b - a}$$

The adjustment factors for the rectangular block samples can be calculated as 1.21 (B_1–B_8), and for two trapezoids as 1.22 (B_9) and 1.23 (B_{10}). Although these factors are not very different, it is clear that air loss will be proportionately higher in the smaller blocks.

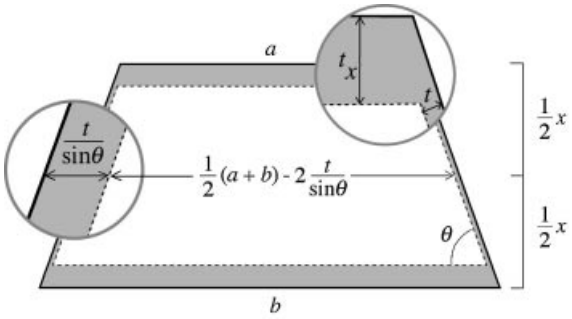

Fig. 5. The calculated adjustment for a 'trapezoidal' sample (B_9 and B_{10}). The shaded area represents the effective surface layer thickness from which air is lost due to water invasion. The adjustment for air loss is calculated from the difference in the volumes of the inner and outer trapezoids based on average dimensions of *a*, *b*, and *x* measured in a number of samples.

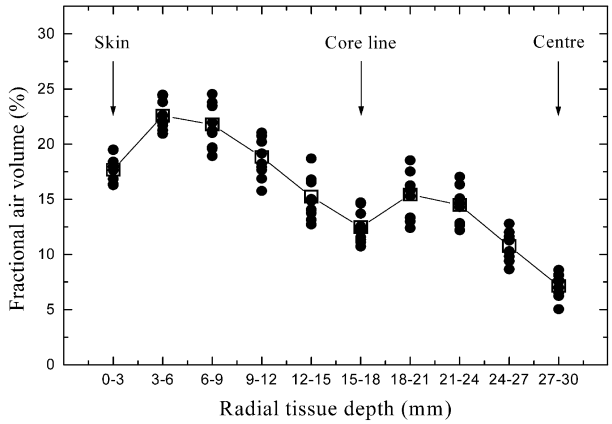

Fig. 6. Changes in fractional air content along a radius in 'Braeburn' fruit. Ten tissue blocks (B_1–B_{10}) were measured sequentially between the fruit surface (0–3 mm) and the centre (27–30 mm). Mean values (squares) are calculated from 10 measured values (circles).

Spatial distribution of intercellular spaces

With the data adjusted for the small air losses suffered on water immersion, a more accurate picture of radial air distribution in the fruit emerged (Fig. 6). Changes in the air content followed a distinct pattern in the cortex and this pattern was repeated in the pith. These two concentric fleshy tissues originate from different parts of the flower (Esau, 1977). In the cortex, the air fraction first increased from a subepidermal level of about 18%, to reach a peak of about 23% in the layer just beneath. It then felt steadily to about 12% at the core line. Here, at the boundary between cortex and pith, a sharp discontinuity occurred with the air fraction rising suddenly to about 15% before falling steadily again to about 7% at the centre of the fruit. All these changes in slope were significant (P <0.001) and all fruit showed a similar pattern but individual fruit intercepts differed (P <0.001).

Discussion

Timings

The air measurement method described here involves the removal of air from the flesh sample and its replacement by water. It is known that the flow of a fluid is inversely proportional to its viscosity, the viscosity of air at 20 °C being 1.813×10^{-5} Pa s and this is much lower than the value for water of 1.002×10^{-3} Pa s (Nobel, 1999). Hence, air will experience very much less resistance to its outflow than will water to its inflow, which is reflected in the distinct differences in time required for air extraction and for water replacement (compare Fig. 3A and B).

Moreover, an increase in the size of the sample will have an influence on the time taken for each of these flows to run to completion. For example, every increase of block size will *increase* the volume of air that must flow out (or of water that must flow in) while it will *reduce* the steepness of the pressure gradients driving these flows. Again this effect is reflected in the equilibration times of Fig. 3A with larger blocks requiring longer timings.

Cell measurements

Information on cell size, shape, and packing provides an important tool for understanding textural and physiological properties of fruit flesh. Cells from the mid-cortex of 'Braeburn' are prolate spheroids with an aspect ratio (long:short cell diameters) close to 1.5, and mean cell diameter of *c*. 250 μm. This is in close agreement with values for other cultivars (Tukey and Young, 1942; Bain and Robertson, 1951; Khan and Vincent, 1990; Harker *et al*., 1997; Atkinson *et al*., 2001). Furthermore, the flesh cells gradually increase in length and become more aligned towards the fruit interior, which agrees with the pattern seen in a number of other apple cultivars (Bain and Robertson, 1951; Reeve, 1953; Khan and Vincent, 1990; Ruess and Stösser, 1993).

These changes result in the numerous air spaces between the cells becoming increasingly organized deeper into the flesh so as to form distinct radial air channels that strongly contribute to the anisotropy and heterogeneity of apple flesh tissue (Vincent, 1989; Khan and Vincent, 1990, 1993*a*). The differences in the size, orientation, and distribution of the air channels make an important contribution to the textural properties of the fruit (Khan and Vincent, 1993*b*).

Adjustment for air loss

An air:water meniscus is in tension and thus will always tend to minimize its area in order to minimize surface energy. This means that when the cut surface of a block of apple flesh tissue is immersed in water, water will tend to

invade any air-filled cavities in the irregular surface but only where to do so involves a *reduction* in the meniscus area. Correspondingly, water will tend *not* to invade cavities whose shape is such that where to do so the meniscus area is required to increase. Thus, in practice, only air spaces lying close to the surface are invaded when a cut tissue sample is immersed in water, but the majority of the air contained deeper within the tissue remains in place and is thus measured. The air lost from tangential surfaces has been estimated as that contained in a layer of thickness $t = 0.25$ of the average cell diameter, but the exact value is not critical to the estimates made in this paper. For example, if the real value of t was zero or 0.5 cell diameter instead, none of the fractional air volumes shown in Fig. 6 would be in error by more than 0.25%.

However, the radial air channels allow water to penetrate somewhat more deeply in this direction. The model proposed, therefore, accounts not only for all the air displaced around the edges of the block but also from air spaces beneath the cut surfaces that are open to water invasion in the radial direction. Thus for the range of samples (1–6 mm in the radial direction), t_x is observed to change gradually with slice thickness (Table 1). In a 1 mm slice, air loss occurs from around 25% of the radial thickness, whereas for a 6 mm slice, loss occurs from less than 10% of the radial thickness. Not surprisingly, therefore, measurement error is inversely related to block size such that in 1 mm thick slices only 0.79 of the total air volume is recorded, while for 6 mm slices the figure is 0.95 (Fig. 4). Consistent with the degree of spatial resolution required, block sizes should be maximized in order to minimize the impact of air loss on the result.

Spatial distribution of intercellular spaces

In 'Braeburn', a progressive decrease in the volume of intercellular air occurred with increasing depth along a radius (Fig. 6). The decrease was not uniform though, and the transect contained two peaks, one in the cortex and another in the pith with the highest fractional air volumes being recorded just inside the bounding tissues (namely, the skin and the core line). The pattern was similar for each fruit, but the volume of intercellular air differed between the fruit in spite of their relatively uniform size (*c*. 5%). This observation points to a significant fruit-to-fruit variability in tissue aeration that could affect both the respiratory metabolism of the fruit and the oral perception of flesh texture.

Other authors have reported a gradient in the volume of the intercellular spaces along a radius. Their results were obtained by vacuum infiltration of rather large samples that referred to the whole of the outer or inner flesh (Reeve, 1953; Vincent, 1989) or were based on stereological estimates from two-dimensional sections (Soudain and Phan Phuc, 1979; Ruess and Stösser, 1993). In this study, a more direct measurement method was employed, using contiguous sampling of still-turgid tissues with adjustment for air loss around the sample edges.

The pattern of change in air content, with its sharp discontinuity at the core line (Fig. 6), is mirrored by changes in both tissue organization and cell packing. The question now is whether these factors could have functional implications in terms of the physiology of gas transfer in 'Braeburn'. Several lines of evidence indicate that this is indeed the case.

Steep gradients in the concentration of gases have been found between the centre and the skin in 'Braeburn' (Rajapakse *et al*., 1990; Dadzie, 1992) suggesting a heterogeneity of internal atmospheres and thus a degree of gaseous compartmentation. Gas movement will experience a greater resistance to diffusion in a tight-packed tissue, with low air content such as the fruit of 'Braeburn' (Rajapakse *et al*., 1990; Yearsley *et al*., 1997*a*, *b*). Irrespective of whether gas diffusion occurs mainly through the air channels (Solomos, 1987) and/or in a combination with fluid/solid matrix of the flesh (Rajapakse *et al*., 1990), a region of reduced intercellular air content will act to impede gaseous diffusion. A partial diffusion barrier at the core line could further restrict gas exchange and lead to increased CO_2 and lower O_2 in the inner parenchyma.

The internal concentration of respiratory gases is also dependent on the permeance of the skin. The skin acts as the primary barrier to gas diffusion in apple fruit having a 10–20-fold higher resistance than the flesh (Solomos, 1987). 'Braeburn' is known to have higher skin resistance than other cultivars (Rajapakse *et al*., 1990; Dadzie, 1992). Hence, when the skin is intact and the tissue is not water-soaked, diffusional gas flow seems to be dominated by the resistance of the skin.

However, if the tissues suffer a partial loss of membrane functionality such that the air spaces become flooded with water, capillarity dictates that this extracellular fluid will migrate towards the tissue regions containing the smallest air pores. These lie around the core line and near the centre of the fruit (Fig. 6). Flooding of air spaces will effectively seal off the inner tissues to respiratory gas exchange (diffusion in a liquid phase is 10^4 times slower than that in a gas phase; Nobel, 1999). In 'Braeburn' this would cause a sharp rise in the internal partial pressure of CO_2 and a lowering in that of O_2, which could lead to tissue breakdown.

These observations are consistent with a model in which the tight-packed internal structure of 'Braeburn' (particularly at the core line) reduces O_2 and CO_2 diffusion resulting in susceptibility to internal injury. It is suggested that the link may in fact be mediated through patterns of flesh structure (namely, air-space distribution) that are modified by factors in the pre-harvest environment.

Conclusions

The study was undertaken to develop a method so that patterns of intercellular air content and of cell shape, size, and packing within the flesh tissue as a whole could be determined. A gravimetric technique based on Archimedes' principle was developed and refined so that accurate assessments of air content could be made in small plant tissue samples. The method proposed is generally applicable to other fleshy fruits and can be used to further understanding of the relationships between structure, function, and quality development of fruit tissues.

In 'Braeburn', the intercellular air content of the flesh shows a systematic decline between the fruit surface and the centre with a marked discontinuity at the core line. This discontinuity effectively separates the fruit into two concentric parts. The radial decline in air content is accompanied by an increase in the degree of cellular organization towards the centre. Gradients in air content underline the importance of location of flesh samples for air content assessment. They also render relatively meaningless the assumption that an air content measurement made at one point can be taken to refer to the whole fruit.

Acknowledgements

This work was supported by the New Zealand Foundation for Research, Science, and Technology (FRST) and the Agricultural and Marketing Research and Development Trust (AGMARDT). The authors are also grateful to Dr Paul Austin, Ms Kathy Murray, Miss Andrea Leonard-Jones, Mr Doug Hopcroft, and Mr Raymond Bennett for their contributions.

References

Atkinson CJ, Taylor L, Kingswell G. 2001. The importance of temperature differences, directly after anthesis, in determining growth and cellular development of *Malus* fruits. *Journal of Horticultural Science and Biotechnology* **76,** 721–731.

Bain JM, Robertson RN. 1951. The physiology of growth in apple fruits. I. Cell size, cell number and fruit development. *Australian Journal of Scientific Research* **4,** 75–91.

Baumann H, Henze J. 1983. Intercellular space volume of fruit. *Acta Horticulturae* **138,** 107–111.

Calbo AG, Sommer NF. 1987. Intercellular volume and resistance to air flow of fruits and vegetables. *Journal of the American Society for Horticultural Science* **112,** 131–134.

Dadzie BK. 1992. Gas exchange characteristics and quality of apples. PhD thesis, Massey University, New Zealand.

Esau K. 1977. *Anatomy of seed plants*. New York: John Wiley & Sons.

Goffinet MC, Robinson TL, Lakso AN. 1995. A comparison of 'Empire' apple fruit size and anatomy in unthinned and hand-thinned trees. *Journal of Horticultural Science* **70,** 375–387.

Harker FR, Ferguson IB. 1988. Calcium ion transport across discs of the cortical flesh of apple fruit in relation to fruit development. *Physiologia Plantarum* **74,** 695–700.

Harker FR, Hallett IC. 1992. Physiological changes associated with development of mealiness of apple fruit during cool storage. *HortScience* **27,** 1291–1294.

Harker FR, Redgwell RJ, Hallett IC, Murray SH, Carter G. 1997. Texture of fresh fruit. *Horticultural Reviews* **20,** 121–224.

Harker FR, Watkins CB, Brookfield PL, Miller MJ, Reid S, Jackson PJ, Bieleski RL, Bartley T. 1999. Maturity and regional influences on watercore development and its postharvest disappearance in 'Fuji' apples. *Journal of the American Society for Horticultural Science* **124,** 166–172.

Hatfield SGS, Knee M. 1988. Effects of water loss on apples in storage. *International Journal of Food Science and Technology* **23,** 575–583.

Khan AA, Vincent JFV. 1990. Anisotropy of apple parenchyma. *Journal of the Science of Food and Agriculture* **52,** 455–466.

Khan AA, Vincent JFV. 1993*a*. Compressive stiffness and fracture properties of apple and potato parenchyma. *Journal of Texture Studies* **24,** 423–435.

Khan AA, Vincent JFV. 1993*b*. Anisotropy in the fracture properties of apple flesh as investigated by crack-opening tests. *Journal of Materials Science* **28,** 45–51.

Nobel PS. 1999. *Physicochemical and environmental plant physiology*. San Diego: Academic Press.

Rajapakse NC, Banks NH, Hewett EW, Cleland DJ. 1990. Development of oxygen concentration gradients in flesh tissues of bulky plant organs. *Journal of the American Society for Horticultural Science* **115,** 793–797.

Reeve RM. 1953. Histological investigations of texture in apples. II. Structure and intercellular spaces. *Food Research* **18,** 604–617.

Ruess F, Stösser R. 1993. Untersuchungen über das interzellularsystem bei apfelfrüchten mit methoden der digitalen bildverarbeitung. *Gartenbauwissenschaft* **58,** 197–205.

SAS Institute Inc. 2000. *SAS OnlineDoc(rtm), Version 8*. Cary, North Carolina: SAS Institute.

Skene DS. 1966. The distribution of growth and cell division in the fruit of Cox's Orange Pippin. *Annals of Botany* **30,** 493–512.

Solomos T. 1987. Principles of gas exchange in bulky plant tissues. *HortScience* **22,** 766–771.

Soudain P, Phan Phuc A. 1979. La difussion des gaz dans les tissus vegetaux en rapport avec la structure des organes massifs. In: *Perspectives nouvelles dans la conservation des fruits et legumes frais*. Seminaire International, Centre de Recherches en Sciences Appliquées à l'Alimentation, L'Université du Québec à Montreal, Canada, 67–86.

Tu K, De Baerdemaeker J, Deltour R, de Barsy T. 1996. Monitoring post-harvest quality of Granny Smith apple under simulated shelf-life conditions: destructive, non-destructive and analytical measurements. *International Journal of Food Science and Technology* **31,** 267–276.

Tukey HB, Young JO. 1942. Gross morphology and histology of developing fruit of the apple. *Botanical Gazette* **104,** 3–25.

Vincent JFV. 1989. Relationship between density and stiffness of apple flesh. *Journal of the Science of Food and Agriculture* **47,** 443–462.

Volz RK, Harker FR, Hallett IC, Lang A. 2004. Development of texture in apple fruit – a biophysical perspective. *Acta Horticulturae* (in press).

Westwood MN, Batjer LP, Billingsley HD. 1967. Cell size, cell number and fruit density of apples as related to fruit size, position in the cluster and thinning method. *Proceedings of the American Society for Horticultural Science* **91,** 51–62.

Yamaki S, Ino M. 1992. Alteration of cellular compartmentation and membrane permeability to sugars in immature and mature apple fruit. *Journal of the American Society for Horticultural Science* **117,** 951–954.

Yearsley CW, Banks NH, Ganesh S. 1997*a*. Temperature effects

on the internal lower oxygen limits of apple fruit. *Postharvest Biology and Technology* **11,** 73–83.

Yearsley CW, Banks NH, Ganesh S. 1997*b*. Effect of carbon dioxide on the internal lower oxygen limits of apple fruit. *Postharvest Biology and Technology* **12,** 1–13.

Yearsley CW, Banks NH, Ganesh S, Cleland DJ. 1996. Determination of lower oxygen limits for apple fruit. *Postharvest Biology and Technology* **8,** 95–109.